



Changing influence of Antarctic and Greenlandic temperature records on sea-level over the last glacial cycle

Mark Siddall^{a,*}, Mike R. Kaplan^b, Joerg M. Schaefer^b, Aaron Putnam^c, Meredith A. Kelly^b, Brent Goehring^b

^a Department of Earth Sciences, University of Bristol, Bristol, UK

^b Lamont Doherty Earth Observatory, Palisades, NY 10964, USA

^c Climate Change Institute, University of Maine, Orono, ME, USA

ARTICLE INFO

Article history:

Received 23 January 2009

Received in revised form

27 October 2009

Accepted 8 November 2009

ABSTRACT

We use a simple model to analyse the relationship between ice core temperature proxy data and global ice volume/eustatic sea-level data over the last glacial cycle (LGC). By allowing the temperature forcing to be a mix of Greenlandic and Antarctic signals we optimise the proportion of this mixing to fit sea-level data. We find that sea-level forcing is best represented by a mix of Antarctic and Greenlandic temperature signals through the whole glacial cycle. We suggest that a distinct bipolar switch occurs which links eustatic sea-level more closely with the Antarctic-like variability during the glacial period (MIS 4, 3 and 2) and more closely to the Greenland-like variability during the last termination (TI) and the interglacial periods (Holocene and MIS 5). This switch may be caused by the spatio-temporal distribution of ice sheet collapse perhaps linked to glacial to interglacial changes in deep water distribution in the ocean, which in turn drive changes in pole-ward heat and moisture transport.

© 2009 Elsevier Ltd. All rights reserved.

1. Introduction

Considerable progress has been made in understanding the history of global ice volume over the last glacial cycle (LGC) (Figs. 1 and 2) (Bard et al., 1996; Flemming et al., 1999; Hanebuth et al., 2000; Yokoyama et al., 2000; Chappell, 2002; Waelbroeck et al., 2002; Siddall et al., 2003, 2004, 2008a,b; Bintanja et al., 2005; Thompson and Goldstein, 2005, 2006; Peltier and Fairbanks, 2006; Arz et al., 2007; Rohling et al., 2008). Although insolation forcing must be an important aspect of the complete climate system it cannot, on its own explain the complicated nature of the glacial cycles, rather any theory linking insolation to the glacial cycles must rely on a sophisticated system of climate feedbacks and interactions (Paillard, 2001). Rather than attempt a complete climate model we make the simplifying assumption that the most direct control on sea-level is temperature. Questions remain about the temperature variability which forced ice sheet growth, decay and fluctuation. Whether these changes in ice volume followed a temperature forcing predominantly like Greenlandic or Antarctic temperature variability (Figs. 1a,b) during and since the glacial period has been a particular focus (e.g. Marshall and Clarke, 1999;

Alley et al., 2002; Bintanja et al., 2002, 2005; Schaefer et al., 2006; Clark et al., 2007). Several authors have discussed the degree to which records of past temperature variability retrieved from Polar regions imply comparable variability for hemispheric or global climates (Denton et al., 2005; Clark et al., 2007).

To further our understanding of these issues we adapt a minimum-complexity model of global sea-level similar to that described first by Rahmstorf (2007), which was developed for applications to the 20th and 21st century sea-level changes. We extend the model to represent the complete glacial cycle. By following a Monte-Carlo approach we are able to explore the model parameter space to ascertain if either the Greenlandic or Antarctic temperature record is capable of describing the variations in sea-level over the last glacial cycle, which are dominated by the growth and decay of the large continental ice sheets. By allowing the temperature forcing to be a mix of Greenlandic and Antarctic signals we vary the proportion of this mixing and evaluate individual simulations against sea-level data, a proxy for global ice volume changes.

2. Model

Our aim is to describe a simple model which can reproduce sea-level estimates when forced by alternative temperature reconstructions. To simplify comparison between temperature

* Corresponding author.

E-mail address: siddall@climate.unibe.ch (M. Siddall).

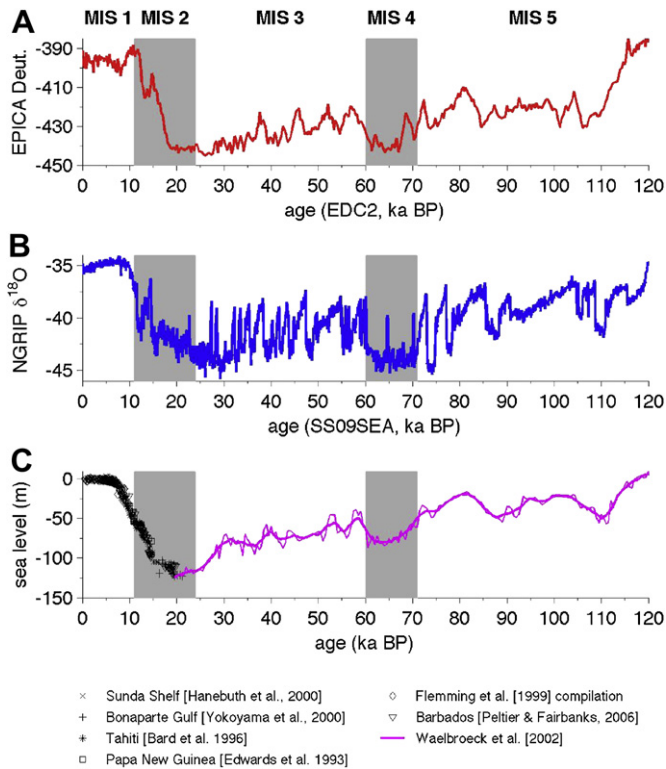


Fig. 1. Temperature data representative of (A) the AA scenario (EPICA Dome C, EPICA Community Members, 2004) and (B) the GL scenario (NGRIP, NGRIP Community Members, 2004). (C) Sea-level data are from Waelbroeck et al. (2002) (purple) except for the last 19 kyr, which are from coral and other benchmark indicators. References for sea-level data shown as black symbols are given in the key. The thin purple line shows the unfiltered Waelbroeck et al. (2002) estimate and the thick purple line shows the data filtered with a five-point running mean. We use the filtered record for the analysis presented in this paper.

proxy records they are expressed in non-dimensional units as $\Delta T'$ so that $\Delta T' = (T - T_{\text{Holocene}}) / \Delta T_{\text{LGM}}$. T_{Holocene} is defined as the mean value between 2 ka BP and the pre-industrial period. Temperature change is expressed non-dimensionally so that $\Delta T'$ is given by dividing ΔT (i.e. $T - T_{\text{Holocene}}$) by ΔT_{LGM} . ΔT_{LGM} is the difference in temperature between the LGM and the Holocene epoch. The LGM temperature is defined as the mean temperature between 25 and 20 ka BP (i.e. we define LGM as between 25 and 20 ka BP). By this definition the Holocene temperature is 0 and the LGM temperature is -1 in non-dimensional units for all of the temperature proxy reconstruction used here. All of the variables used in this paper are summarized and defined in Table 1.

2.1. Equilibrium sea-level

For the purpose of our model we define a theoretical steady state that sea-level would achieve given a stable temperature for a long enough period. We denote this state as 'equilibrium sea-level'. We need to define a function to describe the equilibrium sea-level with respect to temperature change. In order to do this we consider the existing physical understanding of the response of ice sheets to climatic change. These include both positive and negative feedbacks on ice sheet growth (sea-level).

First we consider positive feedbacks. The ice sheet "surface albedo effect" reduces summertime temperatures in the vicinity of the ice sheet, thus minimizing ice sheet ablation and therefore overall ice loss. However, this process also works in reverse as receding ice sheets have a decreased albedo. This surface albedo

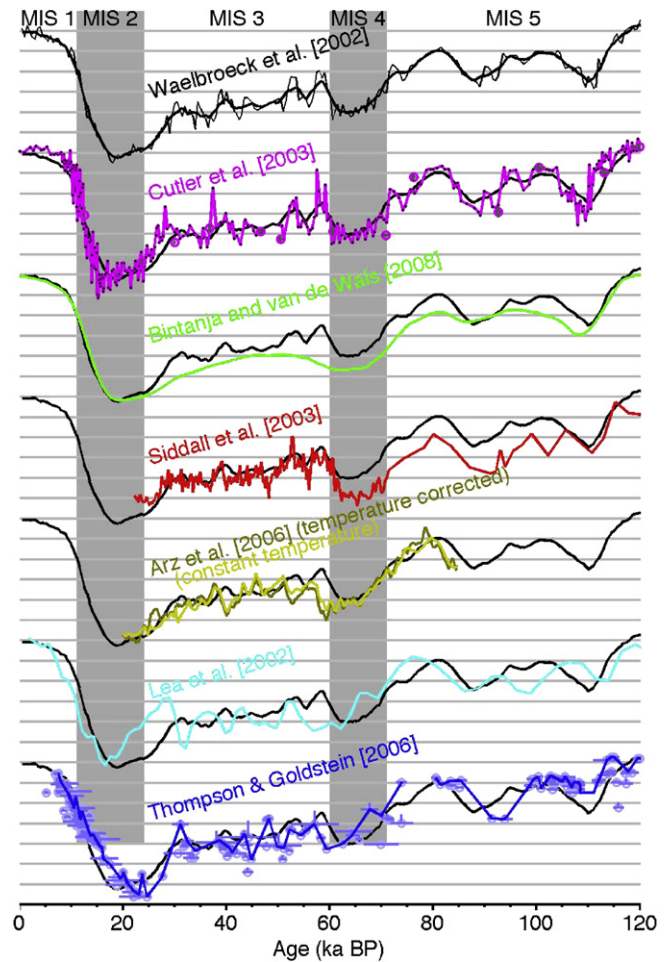


Fig. 2. Comparison of six independent sea-level records with the record of Waelbroeck et al. (2002). Horizontal grey lines are spaced at 20 m intervals to indicate vertical scale. All of the records show very similar structure through the last glacial cycle (LGC) with sea-level low stands during MIS 2 and 4 and relative high stands during MIS 1, 3 and 5.

effect is well documented in many ice sheet models and increases the sensitivity of ice sheets to temperature change (e.g. Oerlemans, 1991; Marshall and Clarke, 1999; Bintanja et al., 2002). A second positive feedback relates to the height of the ice sheet. As the ice sheet elevation increases, the area over which snow can accumulate also increases. This drives a feedback that increases the sensitivity of global ice volume to temperature change during glacial transitions and is also a feature that is reproduced in many ice sheet models (e.g. Oerlemans, 1991; Marshall and Clarke, 1999; Bintanja et al., 2002).

Now we consider the contrasting, negative feedbacks which become significant during periods of maximum ice sheet extent (low sea-level) and tend to stabilise the relationship between temperature and sea-level. The latitudinal temperature increase toward the equator implies that the northern ice sheets have lateral limits on their growth. Support for this negative feedback is given by the knowledge that ice sheets tend to nucleate at high latitude and grow equatorward towards given limits. This pattern of growth is observed in evidence from glacial deposits (e.g. Lowell, 1995; Dyke et al., 2002) and has been reproduced in models (e.g. Oerlemans, 1991; Marshall and Clarke, 1999; Bintanja et al., 2002). As well as lateral limits, ice sheets have vertical limits: snow accumulation on ice sheets decreases at very high elevations. This is a well documented phenomenon known as the elevation-desert

Table 1
Description of variables.

Variable	Description	Unit ^a	Range ^b	Source ^b
<i>Prescribed sea-level variables</i>				
<i>t</i>	Time	kyr	0–120	–
<i>S_{LGM}</i>	LGM sea-level	m	–120 to –140	1
<i>S_{LIG}</i>	LIG sea-level	m	3–6	2
<i>S_{MIS 3}</i>	MIS 3 sea-level	m	–40 to –90	3
<i>S_{MIS 5c}</i>	MIS 5c sea-level	m	–14 to –17	4
<i>S_{proxy}</i>	Proxy sea-level	m	–140 to 5	5
<i>Prescribed temperature variables</i>				
<i>T</i>	Temperature	°C	–	6
ΔT	$(T - T_{\text{Holocene}})/\Delta T_{\text{LGM}}$	–	–	–
ΔT_{LGM}	$T_{\text{Holocene}} - T_{\text{LGM}}$	°C	3.3–5.1	7
ΔT_{LIG}	$T_{\text{LIG}} - T_{\text{Holocene}}$	°C	1.5–2.5	8
<i>p</i>	Proportion of GL versus AA signal in the mixed scenario, M	%	–	–
<i>Model variables</i>				
<i>b</i>	Slope of equilibrium sea-level curve	–	0–0.02	–
<i>c</i>	Variable in Eq. (1)	–	0.5–1	–
τ	Sea-level response time	kyr	1–5	–
<i>r</i>	Ratio of sea-level fall to rise	–	0–1	–
<i>Scaled variables</i>				
<i>A</i>	Scaling of equilibrium sea-level curve	m	–	–
<i>d</i>	Adjustment of equilibrium sea-level curve	m	–	–
<i>Calculated values</i>				
<i>S_e(ΔT)</i>	Equilibrium sea-level at ΔT	m	–	–
<i>S_m(<i>t</i>)</i>	Model sea-level at time <i>t</i>	m	–	–

1. Fairbanks (1989), Yokoyama et al. (2000). 2. Muhs (2002), Stirling et al. (1998). 3. See Siddall et al. (2009d). 4. Schellman and Radtke (2004). 5. See Fig. 5. 6. See Fig. 5. 7. PMIP2 model estimates, see IPCC (2007). 8. IPCC (2007), Masson-Delmotte et al. (2006) using 2× polar amplification (e.g. Hansen et al., 2007).

^a A dash indicates that the variable is dimensionless.

^b The range and source are cited here only if they are prescribed. The Monte–Carlo simulations described here are within the stated range of the prescribed variables shown in bold. Unprescribed variables are generated by the model tuning. The results in this paper are reproducible without prior knowledge of these variables and they are not reported here.

effect (e.g. Budd and Smith, 1979; Oerlemans, 1991; Marshall and Clarke, 1999; Bintanja et al., 2002).

Based on these positive and negative feedbacks, we conclude that the response of sea-level equilibrium to temperature change is greatest during glacial transitions and lower during glacial maxima and minima. Thus, we deduce a sea-level curve that has the gentlest slope during cold and warm periods and the steepest slope during intermediate periods. Therefore, we represent the equilibrium sea-level (S_e) as a function of the inverse hyperbolic sin (\sinh^{-1}):

$$S_e = A \sinh^{-1} \left(\frac{\Delta T' + c}{b} \right) + d, \quad (1)$$

where *b* controls the slope of S_e with respect to $\Delta T'$ and *c* controls the midpoint of the transition in S_e with respect to $\Delta T'$. We vary *c* and *b* and then scale *A* so that S_e gives the correct magnitude of change at the LGM (Fig. 1). The LGM sea-level (S_{LGM}) is therefore an additional scaling factor in the model. We vary S_{LGM} between –140 and –120 m (Fairbanks, 1989; Yokoyama et al., 2000). The variable *d* is adjusted so that S_e passes through the Holocene value (i.e. ~0 m). We vary *b* so that S_e passes through the sea-level estimates for the Last Interglacial (LIG; ~125 ka BP) (Fig. 1). The only completely independent variable in Eq. (1) is therefore *c*. The variable *c* controls the midpoint of the \sinh^{-1} function and it allows the S_e to pass through the range of temperature during the glacial to interglacial transition. In summary, the variables input to the Eq. (1) are S_{LGM} and *b* the other the variables are tuned.

Fig. 3 shows the best 100 of 5000 equilibrium sea-level curves that are used in this paper based on a least-squares analysis. We note that the \sinh^{-1} function used here (Eq. (1)) pass through several independent constraints on equilibrium sea-level (MIS 3 and 5c), indicating that Eq. (1) is supported by the available proxy estimates for our range of Monte–Carlo simulations.

The response of equilibrium sea-level to temperature change suggested by eqn.1 and illustrated in Fig. 3 has interesting properties supported by observational evidence:

(A) Note from Eq. (1) and Fig. 3 that sea-level (i.e. predominantly ice volume) is most sensitive to temperature for intermediate sea-levels (–40 to –100 m sea-level) between stadial and interstadial minima and maxima. Oppo et al. (1998) and McManus et al. (1999) noted that millennial ice rafted debris pulses were present in the North Atlantic ocean sediments coincident with a distinctive range of benthic oxygen isotope values in their sediment core. This range in the benthic oxygen isotope record corresponds closely to the most sensitive part of the sea-level/temperature curve described here, which is indicated by the grey band on Fig. 3. Siddall et al. (2007) noted a period of millennial variability in the Vostok ice core during MIS 8, which was also within this range of high sea-level sensitivity to temperature. The coincidence of ice rafted debris with millennial climate variability suggests a link between ice sheet instability and millennial climate variability (e.g. Hemming, 2004). Eq. (1) suggests that the sensitivity of sea-level to temperature change at intermediate sea-levels may explain why millennial variability is limited to this same sea-level range. Within this range ice sheets are relatively unstable, producing rapid iceberg discharge and provoking millennial variability. Outside this window the sea-level, i.e. ice sheet response to temperature change is limited and ice sheets are relatively stable.

(B) Although Quaternary climate fluctuated greatly during glacial periods, sea-level maxima during successive interglacial periods vary by less than only ~10 m (Martinson et al., 1987; Shackleton et al., 1990; Pirazzoli et al., 1991; Murray-Wallace et al., 2002; Siddall et al., 2003; Rohling et al., 2009). This is also true for sea-level during glacial minima (Martinson et al., 1987; Shackleton et al., 1990; Rohling et al., 1998; Rohling et al., 2009). Eq. (1) implies the inference that the similarity between individual sea-level highstands and lowstands is due to the reduced sensitivity of sea-level to temperature change during peak interglacial and glacial maximum periods throughout the late Quaternary.

The qualitative support explained in (A) and (B) increase our confidence in the ability of our dynamical arguments to represent the response of sea-level equilibrium to temperature change.

2.2. The time scale of sea-level response

Next we define a response time, τ (in units of kyr), which defines the rate at which the modeled sea-level (S_m) rises in response to an increase in S_e in a similar fashion to Rahmstorf (2007), so that at time *t*:

$$\frac{dS_m}{dt} = r \cdot \frac{1}{\tau} \cdot [S_e(\Delta T'(t)) - S_m(t)] \quad \begin{cases} r = 1, & \text{if } S_e(\Delta T'(t)) > S_m(t) \\ 0 < r < 1, & \text{if } S_e(\Delta T'(t)) < S_m(t) \end{cases} \quad (2)$$

The factor *r* accounts for the fact that sea-level rise due to ice sheet decay is faster than sea-level fall due to ice sheet growth (Weertman, 1964). In Eq. (2) *r* is varied between 0 and 1 so that the sea-level rise is fastest (i.e. over a response time τ) following a period of large warming, while any response to rapid cooling occurs over a longer response time (i.e. over a response time τ/r).

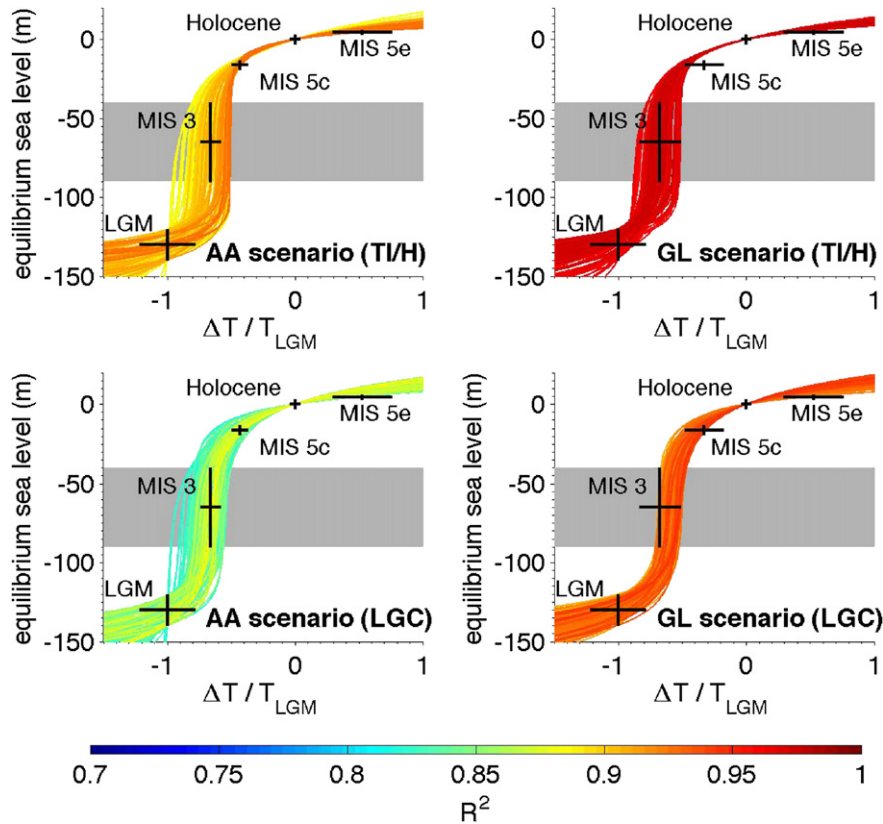


Fig. 3. The equilibrium sea-level curves for the best hundred of 5000 simulations as a function of $\Delta T'$ where $\Delta T' = (T - T_{\text{Holocene}})/\Delta T_{\text{LGM}}$. GL and AA scenarios are given as compared to TI/H (19 ka BP to pre-industrial) and the LGC (120–19 ka BP) as labelled (see Table 1 for definitions). The crosses are observational estimates during periods that may have been close to equilibrium sea-level, except MIS 3 where the box represents the range of variability over that period (see Table 1 for values and references). Temperatures either represent values presented in Table 1 (LIG, LGM) or the mean and standard deviation of the variability in NGRIP and EPICA Dome C combined over the respective periods (Holocene = 7–0 ka BP, MIS 3 = 60–30 ka BP and MIS 5c = 105–100 ka BP). Sea-levels represent published estimates (see Table 1). MIS 3 and 5c values are not used to constrain the model but are simply shown here for comparison. The curves are constrained to pass through Holocene, LGM and LIG values. Equilibrium sea-level is given relative to pre-industrial values. The colour scale gives the R^2 value for each of the simulations/periods shown. The grey horizontal band indicates the range of sea-level in which millennial variability occurs (Oppo et al., 1998; McManus et al., 1999; Siddall et al., 2007).

The time constant τ is varied between a value of 1 and 5 kyr to cover a reasonable range of ice sheet response times.

It is not possible to solve Eq. (2) in closed form because r varies between periods of sea-level increase and decrease. Therefore, sea-level is given by integrating (2) over time step $\Delta t = 0.1$ kyr so that:

$$S_m(t + \Delta t) = S_m(t) + r \cdot \frac{\Delta t}{\tau} \cdot [S_e(\Delta T'(t)) - S_m(t)] \quad (3)$$

where r takes the appropriate value depending on the sign of $S_m(t) - S_e(\Delta T'(t))$. The precise value of Δt that is used has no impact on our results.

The free parameters in Eq. (3) are r and τ . The model does not show a strong sensitivity to the value of r and therefore the dominant parameter in Eq. (3) is τ (see sensitivity tests in Siddall et al., 2009a). Because the variables in Eq. (1) are constrained by observations except for c this means that there are essentially only two significant free parameters in the model: the response time τ and the midpoint of the equilibrium sea-level curve, c . Given the relatively small number of free parameters in the model we do not consider that it is overfitted.

3. Data and simulations

To understand the model response, it is important to develop a clear understanding of the characteristic temperature variability that drives the model, as well as the sea-level estimates against

which the model is evaluated (Fig. 1). First we discuss the sea-level data.

3.1. Sea-level data

3.1.1. The termination and Holocene (19 ka BP¹–present)

Observational constraints for (TI/H) (Fig. 1c), here defined as the period since 19 ka BP, are based on indicators of past sea-level from sites distant from the major ice sheets (so-called ‘far-field’ sites, see e.g. Lambeck et al., 2002). Sea-level indicators such as fossil corals or other depth-dependent coastal deposits reflect isostatic effects associated with the ice-water surface mass redistribution as well as variations in global (eustatic) sea-level. Sea-level indicators at far-field sites are dominated by eustatic effects during the last deglacial sea-level rise (Fleming et al., 1998; Milne et al., 2002; Bassett et al., 2005). In the early Holocene, however, rates of eustatic sea-level rise were reduced and isostatic effects were relatively strong (Lambeck et al., 2002). For these reasons, we use estimates of sea-level from far-field sites uncorrected for isostatic effects for times prior to 9 ka BP (i.e. during TI), and the isostatically corrected far-field dataset of Flemming (1998) for times since 9 ka BP (i.e. during the Holocene). By considering several disparate far-field sea-level records (Bard et al., 1996; Flemming et al., 1998;

¹ Here BP will refer always to calendar years before 1950.

Hanebuth et al., 2000; Yokoyama et al., 2000; Peltier and Fairbanks, 2006), our data set does not include significant biases related to isostatic effects from any particular sample location.

For the period between 120 and 20 ka BP isostatic corrections to benchmark indicators are more difficult to calculate and there is only a limited availability of closed-system U/Th coral ages (Cutler et al., 2003). Open-system effects on U/Th coral dates may be corrected, resulting in a more complete fossil coral sea-level record (Thompson and Goldstein, 2005, 2006). However, even this more complete dataset does not provide a continuous, stratigraphic context for sea-level variability during the LGC. Instead we opt to use a continuous record of variability based on the benthic oxygen isotopes record prior to 20 ka BP (Fig. 1c), as discussed in the next section.

3.1.2. The last glacial cycle excluding TI/H (LGC, 120–20 ka BP)

The broad stratigraphic structure of sea-level variation over the LGC has been known for some time. The SPECMAP project (Imbrie et al., 1984) defined periods of relatively low sea-level by reference to stacked records of oxygen isotopes as recorded in benthic foraminifera. MIS 1 (the Holocene Epoch), MIS 3 and 5 were periods of relatively high sea-level over the last 120 ka, while sea-level was low during MIS 2 and 4 (Waelbroeck et al., 2002; Cutler et al., 2003; Siddall et al., 2008a). Many independent sea-level records corroborate this broad structure of eustatic sea-level change over the last glacial cycle (e.g. Siddall et al., 2007, 2008a). Here we will use the sea-level estimates for the LGC based on the scaling of benthic isotopes to sea-level by Waelbroeck et al. (2002), though we also demonstrate that our result is not sensitive to the choice of benthic isotope records that we apply.

The approach of Waelbroeck et al. (2002) largely overcomes the limitations of the benthic oxygen isotope record as a proxy of sea-level. We refer readers to Waelbroeck et al. (2002) for a more complete explanation. Here we present a brief outline. Benthic oxygen isotopes do not show a simple linear response to ice sheet growth. For example there is a fractionation due to temperature at the point that oxygen isotopes are incorporated into the tests of benthic foraminifera (Shackleton, 1974) so that benthic isotope records represent a conflagration of information regarding deep ocean temperature and global ice volume. For this reason Waelbroeck et al. (2002) applied a polynomial scaling to the benthic isotope record directly to sea-level estimates based on U/Th dated fossil coral reef data, which are independent of deep sea temperature. Importantly, by scaling the benthic isotope record to an extensive set of coral reef data the Waelbroeck et al. (2002) record is informed by much of our existing knowledge of sea-level variation throughout the last glacial cycle. Seawater isotopic composition is known to lag ice volume by several thousand years due to the 'legacy effect' described by Mix and Ruddiman (1984). Essentially, the mean isotopic composition of an ice sheet is not a constant but changes through time due to the fact that the initial snowfall that builds an ice sheet occurs typically close to sea-level, and so is relatively isotopically heavy. As the ice sheet builds and gains elevation, the isotopes become more and more depleted so that after tens of thousands of years, the cores of major ice sheets are highly depleted. During deglaciation, it is the margins that melt first, with heavy isotopes, and only much later the highly depleted isotopes at the cores of the ice sheets are melted. To overcome the 'legacy effect' Waelbroeck et al. (2002) applied separate scalings for the glaciation and the deglaciation, demonstrating the hysteresis between the benthic isotope record and sea-level during the last glacial cycle. Local hydrography is known to have important effects on benthic isotope values in the Atlantic and Indian Ocean basins (e.g. Lear et al., 2000; Waelbroeck et al., 2002). The Waelbroeck et al. (2002) sea-level estimates used here make use of benthic

isotope records from the deep Pacific. The deep Pacific is the largest and least dynamic of any of the ocean basins and it is commonly assumed that the deep Pacific is not subject to large hydrographic variations during the glacial cycle. In this regard, the deep Pacific should be relatively unaffected by changes in hydrography.

To check the reliability of the Waelbroeck et al. (2002) sea-level reconstruction we compare it to five independent records of sea-level change during the last glacial cycle (Fig. 2). Fig. 2 shows sea-level estimates based on: (1) Red Sea oxygen isotope ratios (Siddall et al., 2003; Arz et al., 2007); (2) a compiled coral record (corrected from open-system effects on U/Th ages) (Thompson and Goldstein, 2005, 2006); (3) an alternative scaling of the benthic oxygen isotope record (Cutler et al., 2003) to coral indicators; (4) an inverse model of changes in benthic oxygen isotope values based on the calculation of temperature and isotope fractionation due to the growth of the Fenno-Scandian and North American ice sheets (Bintanja and van de Wal, 2008); and (5) a record based on oxygen isotope records from the Equatorial Pacific with the temperature component removed using Mg/Ca temperature reconstructions (Lea et al., 2002). For reference we compare each to the benthic isotope compilation of Waelbroeck et al. (2002) which was scaled to fossil coral reef sea-level indicators. There are considerable similarities between each of these records in terms of the magnitude and stratigraphy of the sea-level variability. Therefore, we are confident that no significant bias exists in our approach as a result of our choice of sea-level record.

In summary Fig. 2 demonstrates that the use of the Waelbroeck et al. (2002) record does not bias our results and that their reconstruction is representative of other published estimates. We choose this record because it is continuous through the last glacial cycle as well as benefiting from the available fossil coral reef data (to which the Waelbroeck et al., 2002 estimate was scaled). The continuity of the record gives it a strong stratigraphic context (which is sometimes missing from coral reef data in the absence of reef growth models) and best suits the Monte–Carlo approach we employ here. Because the comparison with other sea-level reconstructions is favourable we assume that the uncertainty associated with this record is stochastic (associated with individual data points) and not systematic (associated with systematic trends in the difference with the other reconstructions). For this reason we do not consider uncertainty in the sea-level reconstruction in this paper. Instead we concentrate on uncertainties in the variable associated with our model which are more significant to our conclusions.

3.2. Temperature data

We use temperature data from Antarctic and Greenlandic ice core records, described further below, to simulate sea-level records for the last glacial cycle. We recognize that there are uncertainties in using both Antarctic and Greenlandic temperature proxy records. Our objective is to present a new approach to evaluate which of the two scenarios might provide insight into the different forcings of sea-level over the last glacial cycle.

3.2.1. The scenario forced by Antarctic temperature ('the AA scenario')

We underline that in using Antarctic temperature in our sea-level model we are not assuming that large proportions of the glacial to interglacial range in sea-level originated from the Antarctic ice sheet. Rather we are investigating the extent to which the temperature variability found in Antarctic temperature records represents variability at sites distant from Antarctica, as argued by Clark (2002c), Clark et al. (2007).

We define Antarctic temperature using the EPICA DOME C deuterium record (EPICA Community Members, 2004). The EPICA

DOME C record is the most recent of a series of ice core temperature proxy records developed from Antarctica (Blunier et al., 1998; Blunier and Brook, 2001; Petit et al., 1999; Brook et al., 2005; EPICA Community Members, 2006; Kawamura et al., 2007). The similarity between the EPICA DOME C record and other Antarctic temperature records is striking, and suggests that the temperature signature recorded by Antarctic ice cores represents a wide geographical area (Vimeux et al., 2001; EPICA Community Members, 2004; Jouzel et al., 2007). A recent study used a coupled GCM model to suggest that the EPICA deuterium proxy may represent the climate of large areas of the Pacific Ocean (Jouzel et al., 2007). Clark (2002c), Clark et al., 2007 considered the extent to which the Antarctic ice core proxies can be considered a 'global signal,' and gave the label 'southern mode' to temperature changes inferred from the Antarctic ice cores. We refer to this situation as the 'AA scenario,' whereby global ice volume is forced by the EPICA Dome C temperature reconstruction. Because Antarctic-like mode of climate variability is found in many climate proxies which are sensitive to changes in different seasons across a broad swathe of the planet (Clark 2002c, Clark et al., 2007) we assume that the D–O events affect both annual average and seasonal temperatures.

Bintanja et al. (2005) ran an inverse model to calculate temperature and ice volume from the benthic oxygen isotope record. The temperature record generated in this way bears a striking similarity to the Antarctic temperature record, indicating that it is the Antarctic temperature variation that closely reflects ice volume variation during the last million years. However, the Bintanja et al. (2005) model did not consider millennial variability, or the last glacial cycle in detail. Instead, this study focused on multiple glacial cycles rather than the specific details of variability within the glacial cycles.

Clark et al. (2007) provided an additional argument in support of the 'AA' scenario. They suggested that sea-surface temperatures in the equatorial Pacific, which resemble the Antarctic temperature signature, drove the mass balance of the Laurentide and Fennoscandinavian Ice Sheets. However, whether the AA temperature variability adequately characterized the temperature over the Laurentide Ice Sheet, the major cause of eustatic sea-level change during the glacial cycles, remains a matter of debate (Arz et al., 2007; Rohling et al., 2008).

3.2.2. *The scenario forced by Greenlandic temperature ('GL scenario')*

Temperature fluctuations recorded in the NGRIP ice core are similar to those determined from other ice cores from Greenland, and thus can be taken to represent a broadly regional signal (Andersen et al., 2006; Svensson et al., 2006). For the period since 40 ka BP the various age models for the Greenlandic ice core records are in agreement on the timing of Greenlandic temperature fluctuations (Andersen et al., 2006; Svensson et al., 2006). However, prior to 40 ka BP the age models for the Greenlandic ice core records diverge (Andersen et al., 2006; Svensson et al., 2006). Furthermore, the NGRIP isotope record has been shown to represent the broader 'northern mode' northern hemisphere temperature variability (Clark 2002c, Clark et al., 2007), and includes as the classic abrupt climate changes known as 'Dansgaard–Oeschger' or 'D–O events' (Dansgaard et al., 1984, 1993; Oeschger et al., 1984). D–O events appeared to have an impact on the Asian monsoon (Wang et al., 2001). The spatial extent of this signal has been considered in detail by Denton et al. (2005) and Clark (2002c, Clark et al., 2007). Schmittner et al. (2003), Stocker and Johnsen (2003) and the EPICA team (2006), among others have also suggested that D–O variability propagates into the southern hemisphere as a lagged and damped signal of opposite sign, as recorded in the Antarctic ice core record. Greenland is situated close to the former

limits of the Laurentide and Fennoscandinavian Ice Sheets, and thus Greenlandic ice core temperature records have been used in multiple studies (e.g. Marshall and Clarke, 1999; Bintanja et al., 2002; Johnson and Fastook, 2002) to drive northern hemisphere ice sheet models. We label this scenario, which is driven by the NGRIP temperature record, the 'GL scenario'. Because the D–O events are found in many climate proxies which are sensitive to changes in different seasons across a broad swathe of the planet (Clark 2002c, Clark et al., 2007) we assume that the D–O events affect both annual average and seasonal temperatures in gross terms. Note that we are concerned with the gross characteristics of the D–O events, rather than more subtle, local and seasonal differences.

The interaction between sea-level fluctuations and the D–O events has been the focus of much debate (see Siddall et al., 2008b for a recent summary). Cold D–O stadials are generally considered to be themselves caused by iceberg discharge related to ice sheet dynamics (e.g. Hemming, 2004). It may be incorrect to use a temperature record which is possibly affected by ice sheet instability to simulate ice sheet growth. It has been pointed out by Knutti et al. (2004) and Siddall et al. (2008b) that the duration of the D–O stadials is proportional to the amplitude of sea-level rise which may be associated with each stadial. Similarly the duration of the D–O stadials is proportional to the amplitude of Antarctic warming which may be associated with each stadial (Stocker and Johnsen, 2003; EPICA, 2006). In summary, both Antarctic temperature and sea-level scale according to the duration of the D–O stadials so the D–O stadials can be explained if sea-level rise is driven by Antarctic-like temperature variability. This possibility is accounted for in the AA and mixed scenarios described in this section.

A comment is required on the effect of seasonal biases in the GL scenario. Denton et al. (2005) suggested that mean-annual temperatures inferred from Greenlandic ice cores were weighted towards extremely cold winter temperatures during abrupt stadial events. Because summer temperatures affect the melting of ice sheets Denton et al. (2005) consider them to be relatively more important than winter-time temperatures for ice sheet mass balance. Therefore, the argument of Denton et al. (2005) suggests that the GL scenario may not be necessarily the most appropriate record to use to represent the sea-level (ice volume) forcing during this period of time – GL temperature reconstructions may not be representative of the summer time temperatures which are a key influence on ice sheet mass balance. However, Denton et al. (2005), make this conclusion tentatively because of the large diversity of marine and terrestrial proxy records in the northern hemisphere which contain pronounced D–O variability. Indeed temperature reconstructions which do not contain the strong seasonal bias outlined by Denton et al. (2005) also contain a strong signal of D–O variability with similar large amplitude to the GL records (e.g. Shackleton et al., 2000; Pailler and Bard, 2002).

3.2.3. *The mixed scenario*

We consider a third alternative that mixes varying proportions of the AA and GL scenarios. We call this the 'mixed scenario'. This approach is useful because, for example, it allows for the suggestion of the GL record being strongly biased by winter temperatures (Denton et al., 2005) by effectively reducing the magnitude of the GL forcing relative to that of AA. Clark et al. (2007) consider EOF analyses of many globally distributed climate records and find that a significant number of these can be described as a mix of northern and southern mode influences (i.e. AA and GL scenarios) indicating that our mixed scenario is physically reasonable. Clark et al. (2007) point out that both AA and GL scenarios actually share some aspects in common and are not simply 'end members' of the climate system. Barker and Knorr (2007) identify a clear AA signal in the GL

variability by removing the step-like jumps in temperature in the GL signal. Most significantly for last glacial termination (Alley et al., 2002) and for the last four glacial terminations (Paillard, 2001), the initial warming is synchronous in both the GL and AA records until the rapid warming of the northern hemisphere at the Bolling–Allerød. We note therefore that this mixed scenario has a strong basis in existing observations and previously published conclusions.

To consider the relative influence of GL and AA scenarios on global sea-level both the NGRIP and EPICA Dome C we define a new mixed record, ΔT_M . This synthetic temperature record is defined according to a constant mixing proportion, p , between 0 and 1 so that: $\Delta T_M = p\Delta T_{GL} + (1 - p)\Delta T_{AA}$. The mixing proportion p is an additional model variable in the mixed scenario.

3.3. Simulations

We analyse two time periods using the model. We extend the analysis of TI/H (20 ka BP–present) first presented by Siddall et al. (2009a) to include the mixed scenario and also consider the period from the glacial inception until TI (120–20 ka BP). By following a Monte–Carlo approach rather than the least-squares optimisation of Siddall et al. (2009a) we are able to explore the behaviour of the model with respect to a broad range of parameters.

For each scenario we carry out 5000 simulations, randomly varying the free parameters in the ranges given in Table 1. Each parameter is kept constant for the duration of each simulation. Each simulation is evaluated using the coefficient of regression, R^2 . Although R^2 would in most cases show a bias towards the model simulating the amplitude of large changes, in the case of our model the amplitude of glacial to interglacial changes is prescribed by Eq. (1). Therefore R^2 differentiates simulations during periods of change (rather than simply the amplitude of the change). These periods are the focus of our interest. Although R^2 might be expected to be relatively high in each of our simulations because the amplitude of the glacial to interglacial change is prescribed, the difference in R^2 between simulations should reasonably differentiate the more representative simulations.

In summary, for each of the 5000 simulations in each scenario, a new equilibrium sea-level curve, response time and ratio between rising and lowering sea-level are randomly prescribed and evaluated. Optimal solutions are calculated from the mean of the best ten simulations weighted to the R^2 for each simulation.

4. Results

4.1. Termination I and Holocene (TI/H, 20 ka BP–present)

The least-squares optimisation of Siddall et al. (2009b) concluded that the dominant control on sea-level during the glacial termination was the GL mode of climate variability. The Monte–Carlo analysis presented here supports this conclusion (Figs. 3 and 4). For the mixed scenario the optimal solution suggests that there is only a 15:85 ratio of AA:GL influence on the sea-level during TI. Key stratigraphic events in the sea-level curve during TI are well described by the GL scenario (i.e. LGM, Bolling–Allerød, Younger Dryas, Holocene). For example, the model captures a rapid increase in sea-level subsequent to Bolling–Allerød time. This rise slows to a stillstand or even slight ($\ll 10$ m) sea-level drop during Younger Dryas time. Finally, during the rapid warming subsequent to the Younger Dryas, sea-level rises rapidly once more. These events are not well described by the AA scenario.

Unlike later events in the ice core records, the warming between 20 and 15 ka BP is common to both the AA and GL scenario (as noted in Section 2.2.3). In response to this early warming

sea-level starts to rise at 20 ka BP in both scenarios, in agreement with indications from moraine data from the Laurentide Ice Sheet (Denton et al., 1999; Dyke et al., 2002).

4.2. The last glacial cycle (LGC) excluding TI/H (120–20 ka BP)

4.2.1. The complete LGC (120–20 ka BP)

Figs. 3 and 5 show model simulations of the LGC excluding TI/H (120–20 ka BP). These simulations are evaluated and the optimal simulations are found for the mixed scenario with 41:59 ratio of influence of the AA compared to the GL scenario. This differs from TI/H when the optimum solution was found with a 15:85 ratio of influence for AA:GL variability.

The cold period associated with MIS 4 is registered differently by Greenland and Antarctic temperature records. In Greenland, the cold period associated with MIS 4 was longer and colder than in Antarctica (Figs. 1a,b). In fact, the cold period associated with MIS 4 was longer and colder than MIS 2. In contrast, in Antarctica, the cold period associated with MIS 4 was shorter and generally warmer than MIS 2. Sea-level changes during MIS 4 may therefore help to discriminate between the dominant sea-level forcings during the LGC. The long, cold MIS 4 in the GL scenario results in simulated sea-levels which are lower than proxy estimates because the model has more time to equilibrate to an equilibrium sea-level which is lower than that observed (Fig. 5). The comparatively short, warm MIS 4 in the AA scenario (compared to the GL scenario) is more easily reconciled with sea-level proxy estimates during the LGC because the model has less time to equilibrate to a sea-level and the equilibrium sea-level is only a little lower than the observed sea-level. The links between MIS 4 sea-level estimates and Antarctic temperature variability explain in part why sea-level is weighted to the AA scenario during the LGC compared to TI/H.

4.2.2. Varying contributions through the LGC prior to TI/H (120–20 ka BP)

To understand the time-variable influence of Greenlandic and Antarctic temperatures on sea-level, we consider further the LGC in distinct time slices. This allows us to determine whether the influence of the GL versus AA variability varies over the LGC in a systematic fashion. We consider four overlapping phases of the LGC over periods 50 kyr in duration (69–19, 87–37, 103–53 and 120–70 ka BP). These results are shown in Fig. 6.

The period 120–70 ka BP encompasses MIS 5 and is dominated by the influence of the GL scenario (29:71 ratio of influence of AA:GL). The period 103–53 ka BP largely covers MIS 5 but also includes MIS 4 and a portion of MIS 3. The dominance of the GL scenario is similar for this period as for the period from 120 to 70 ka BP (29:71 ratio of influence of AA:GL). The period 87–37 ka BP represents the transitions between MIS 5, 4 and 3. The influence of the GL and AA scenarios are balanced (61:39 ratio of influence of AA:GL). This period represents a transition between a period dominated by GL forcing and a period dominated by AA forcing. The period 70–20 ka BP encompasses MIS 4, 3 and 2 and is dominated by the influence of the AA scenario, although the GL scenario still plays some role (71:29 ratio of influence of AA:GL).

To summarise, the influence of GL and AA variability during the LGC appears to loosely track the MISs. During the interglacial period MIS 5 and T1 (i.e. the transition between MIS 2 and 1) Greenlandic temperature is the dominant control on sea-level variability. However, during the cold stages MIS 4, 3 and the LGM (the early part of MIS 2) sea-level is dominated by Antarctic temperature with some influence from Greenlandic temperature. We term this change between glacial and interglacial/termination conditions the bipolar switch. The bipolar switch occurs when the dominant influence on sea-level 'switches' between Antarctic and

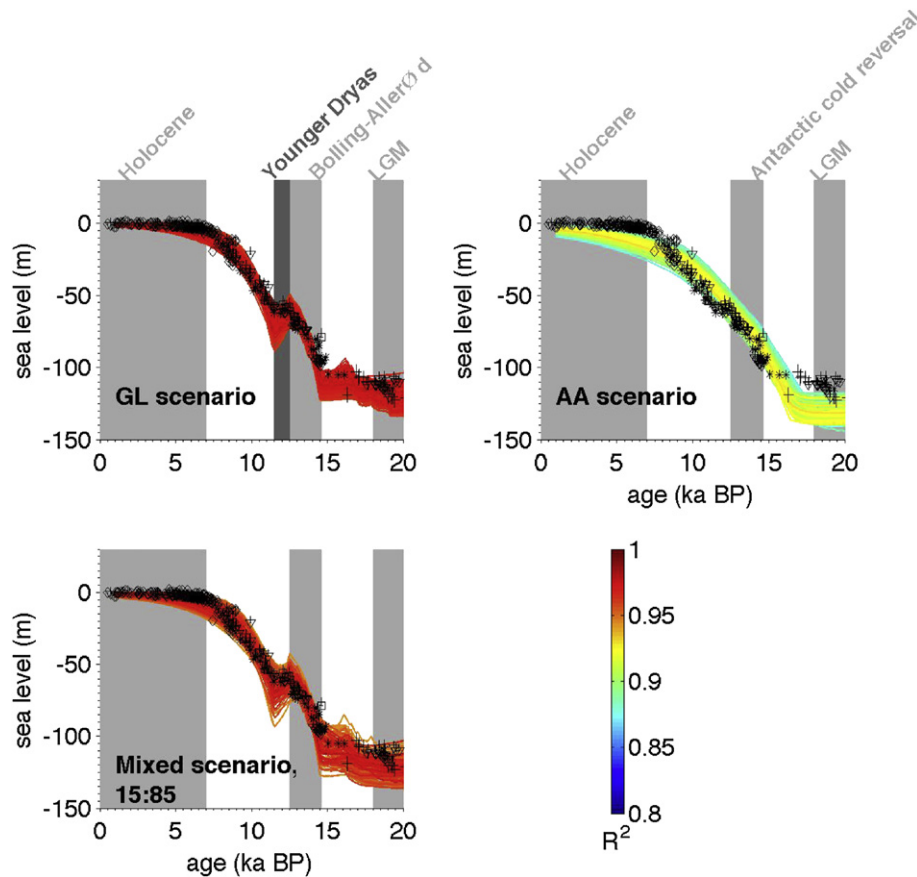


Fig. 4. Model output for best one hundred of 5000 simulations of TI/H for the AA scenario, the GL scenario and mixed scenarios. The colour scale represents the model fit to data, as measured by R^2 . The grey bars represent stratigraphically distinct periods during TI/H as labelled. The sea-level data is shown as the black symbols referenced in Fig. 2c. The ratio noted in the plot of the mixed scenario represents the proportion of the AA scenario affecting the signal compared to the GL scenario. This value is the mean of the best ten simulations weighted to the R^2 for each simulation.

Greenlandic temperature influences. We suggest that this bipolar switch provides insight into the mechanisms that influence the transition between glacial and interglacial climate states.

5. Synthesis and discussion

5.1. Construction of a 'bipolar switch' sea-level model

Given the suggestion for the existence of a bipolar switch in the results presented in Section 4 we construct a scenario for which we evaluate the model differentially depending on the period in question. This scenario represents the mixed scenario in two separate segments. One segment is made up of the interglacial periods and the termination MIS 1, 5 and TI/H. The second segment is made up of MIS 2, 3 and 4. In each of these two segments the proportion of GL versus AA influence differs, as shown in Fig. 7. During the glacial periods the AA scenario dominates (76% of the variability is controlled by the AA scenario) while during the interglacial periods the GL scenario dominates (84% of the variability is controlled by the GL scenario).

This simulation can be regarded as optimal with 95% of the variability in the sea-level estimates presented explained by the model. This represents an improved representation of sea-level estimates over all LGC simulations, and is comparable to the optimal simulations for TI/H.

5.2. Changing influences on ice sheets over the glacial cycle

Previous work on simulating sea-level over the last glacial cycle has often assumed that Greenlandic ice core temperature reconstructions can be used to force ice sheet models (e.g. Marshall and Clarke, 1999; Bintanja et al., 2002). More recently results from modelling the relationship between Red Sea oxygen isotopes and sea-level have suggested that in fact sea-level may respond to AA variability during MIS 3 (Rohling et al., 2008). Other work on the Red Sea has concluded that sea-level responded to GL variability (Arz et al., 2007). We refer readers to Rohling et al. (2008) for a full discussion of recent Red Sea results but here we note that recent evidence brings into question the simple assumption that sea-level responds to GL variability. Indeed, the modelling work of both Clark et al. (2007) (for MIS 3) and Bintanja et al. (2005) (for the last Myr) concluded that ice sheets respond to AA variability. Our results are in broad agreement with these conclusions during the glacial period but we find that ice sheets respond to GL variability differently during the termination. We therefore suggest a more complicated picture where by the influence of AA and GL variability varies through the glacial cycle.

5.3. Causes of the bipolar switch

5.3.1. Characterising the climate states across the bipolar switch

Here we consider evidence of significant differences in the distribution of water masses and changes in the temperature and

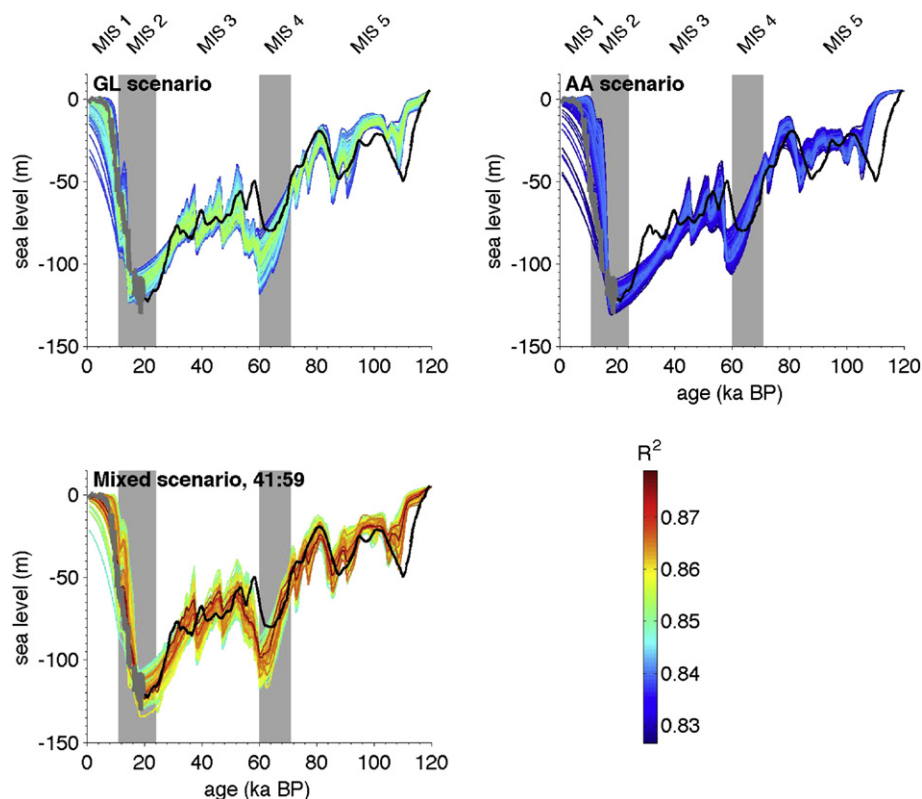


Fig. 5. Model output for best one hundred of 5000 simulations for the AA, GL and mixed scenarios (as labelled). The colour scale represents the model fit to data, as measured by R^2 , evaluated over the LGC (120–19 ka BP). The grey bars represent MIS as labelled. Sea-level estimates from Waelbroeck et al. (2002) are shown as a black line and are used to evaluate the model simulations. The data over TI/H (as shown in Fig. 2c) is shown as a grey line but this is not used to evaluate the model. The ratio noted in the plot of the mixed scenario represents the proportion of the AA scenario affecting the signal compared to the GL scenario. This value is the mean of the best ten simulations weighted to the R^2 for each simulation.

salinity of the deep ocean between glacial and interglacial periods and link these differences to the bipolar switch.

Studies of benthic isotopes in the deep Pacific support the concept of changes to AABW during the glacial period, as will be outlined in this paragraph. By comparing these records to independent sea-level reconstructions several authors have attempted to reconstruct deep ocean temperatures in the deep Pacific during the LGC (Chappell and Shackleton, 1986; Waelbroeck et al., 2002; Cutler et al., 2003). Each of these reconstructions suggests that the deep ocean temperature was stable and approximately 2 °C cooler than the Holocene during the glacial period (MIS 4, 3 and 2) so that the deep Pacific was close to freezing point. Interestingly the transitions in temperature in the deep Pacific coincide with the periods at which we suggest the bipolar switch operates (Fig. 8b). Although temperatures during MIS 5d–5a are close to the glacial cold state they never quite transition to them until the MIS 5a–4 transition. Results comparing sediment pore water oxygen isotopes with oxygen isotopes in benthic foraminifera in the same core confirmed that the deep Pacific was approximately 2 °C cooler during the LGM compared to the Holocene period (Adkins et al., 2002; Adkins and Schrag, 2003). However, this study did not consider the LGC prior to the LGM. If the deep Pacific was indeed close to freezing point during the glacial period this links the deep ocean circulation with changes in sea ice formation in the SO because it results in the formation of deep water masses which are close to freezing point – i.e. deep circulation and sea ice formation in the SO switch at the same moment as the bipolar switch (Fig. 8). But could changes in ocean circulation account for the glacial cycles? Siddall et al. (2009a) recently extended the work of

Waelbroeck et al. (2002) to the last 5 Ma and found that the glacial switch in deep Pacific temperatures coincides with the onset of the Quaternary glacial cycles across the Mid-Pleistocene transition.

Lowell et al. (1995) and Denton et al. (1999) considered the relationship between changes in ocean circulation linked to the bipolar seesaw and the growth of the large continental ice sheets. The bipolar seesaw drives changes in climate which are out of phase between the northern and southern hemispheres (e.g. Alley et al., 2003; Schmittner et al., 2003; Stocker and Johnsen, 2003). They concluded that such asynchronous changes cannot account for the near synchronous deglaciation across hemispheres (e.g. Schaefer et al., 2006). However, the discussion in the paragraphs above suggest that changes in deep ocean circulation linked to the glacial period were not uniquely related to the bipolar seesaw. Instead, observations suggest that the glacial deep ocean circulation was different to modern circulation in many respects and may well have been less efficient at distributing heat to the polar regions in general, regardless of hemisphere.

Mapping of water mass signatures at the LGM shows that NADW shoaled and thinned and became Glacial NADW (GNADW) (Curry and Oppo, 2005). Concurrently, AABW penetrated further north (Curry and Oppo, 2005) and became relatively cold (even close to freezing) (Adkins et al., 2002; Adkins and Schrag, 2003). The residual temperature record from the deep Pacific suggests that the transitions to and from this glacial deep ocean may have occurred at the end of MIS 5 and during TI (Fig. 8b) (Chappell and Shackleton, 1986; Waelbroeck et al., 2002; Cutler et al., 2003). We suggest that the ‘bipolar switch’ occurs at these same periods. This implies that the AA scenario is the dominant influence on sea-level when the

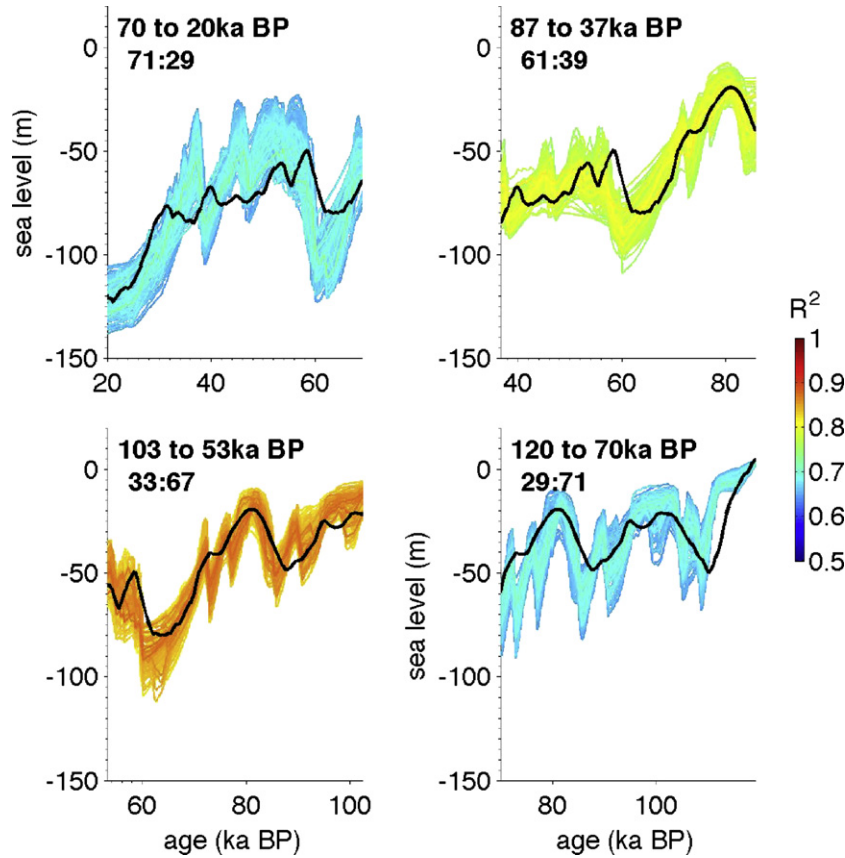


Fig. 6. Model output for best one hundred of 5000 simulations for the mixed scenarios (as labelled). The colour scale represents the model fit to data for each period, as measured by R^2 . The ratios noted in each plot represent the proportion of the AA scenario affecting the signal compared to the GL scenario. These values are the mean of the best ten simulations weighted to the R^2 for each simulation.

ocean circulation is in a glacial configuration and the GL scenario controls sea-level when the ocean circulation is in an interglacial or transitional configuration.

There are similarities between the suggestions in the paragraphs above and those of Denton (2000). Like Denton (2000) we suggest a ‘switch’ between glacial and interglacial states linked to the deep ocean circulation. However, Denton (2000) argued that the GL temperature reconstructions represented the dominant

temperature forcing on sea-level during the glacial period. We suggest that the same deep ocean circulation ‘switch’ which Denton (2000) suggest characterises the interglacial/glacial transitions, also switches the dominant temperature forcing on the ice sheets between GL and AA modes.

Perhaps the clearest indication of a link between ocean circulation and ice sheet formation is suggested by the work of Clark et al. (2007). These authors suggest links between AA variability during MIS 3 and ice sheets via a link between sea-surface temperature in the equatorial Pacific and surface mass balance over the Laurentide Ice Sheet. In turn equatorial Pacific temperatures are suggested to respond to SO temperatures via the upwelling of Antarctic Intermediate Water at the equator. We suggest that this link between SO temperatures and the major ice sheets of the northern hemisphere could also be in effect during MIS 4 and 2 but break during the termination and interglacial period when changes in the North Atlantic dominate.

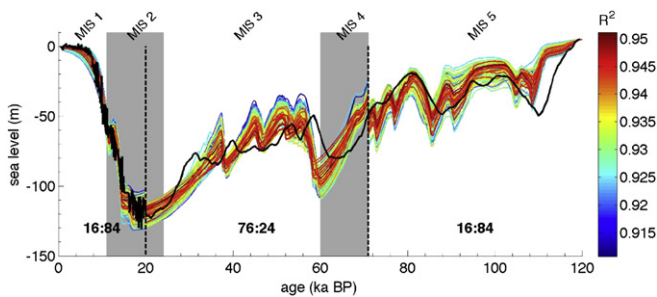


Fig. 7. Model output for best one hundred of 5000 simulations for the optimal scenario (as labelled). This scenario represents the mixed scenario in two separate segments. One segment is made up of the interglacial periods and the termination MIS 5 and TI/H. The second segment is made up of MIS 3 and 4. In each of these two segments the proportion of GL versus AA influence differs. The colour scale represents the model fit to data, as measured by R^2 . The grey bars and labels represent the Marine Isotope Stages (MIS). The ratios noted in each section represent the proportion of the AA scenario affecting the signal compared to the GL scenario. These values are the mean of the best ten simulations weighted to the R^2 for each section.

5.3.2. Triggers for the bipolar switch – insolation and sea ice

The SPECMAP project assigned a time scale to the MISs based on the summer insolation at 65°N (Martinson et al., 1987; Shackleton et al., 1990). That the bipolar switch appears to operate at the transitions between MISs may link the change in GL versus AA influences to changes in orbital parameters driving the climate across some threshold. For example, a threshold forcing at which the bipolar switch operates may be due either to the direct influence of insolation on (northern hemisphere) ice sheet growth or may also be linked to other changes in the ocean/atmosphere system. Here we discuss this possibility.

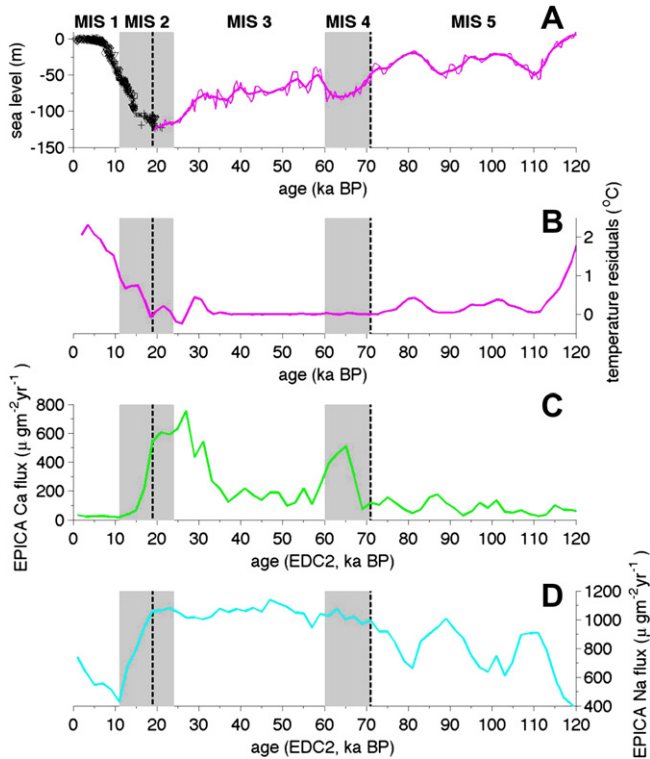


Fig. 8. Time series of data discussed in the text. (A) The sea-level estimates used to evaluate the model as referenced in Fig. 2. (B) The temperature residuals after removing the sea-level component from the benthic isotope record in the deep Pacific (Waelbroeck et al., 2002). (C) Ca flux in the EPICA Dome C ice core record, a proxy for the flux of continental dust (Wolff et al., 2006). The dust in Antarctica has been isotopically linked to a Patagonian source with peak concentrations, possibly corresponding to windblown material produced during glacial periods (Basile et al., 1997). (D) Na flux in the EPICA Dome C record, a proxy for SO sea ice (Wolff et al., 2006).

Hansen et al. (2007) suggested that the termination of glacial periods is linked to variations in sea ice formation in the SO driven by insolation variations at 75°S during the austral spring. It may be the case that such changes engender glacial terminations by driving changes in the Antarctic ice sheet (e.g. Clark et al., 2002a,b; Weaver et al., 2003). Could increases in SO sea ice formation have brought about the glacial advance and driven the bipolar switch? There is evidence to support this claim in the dramatic increase in salt deposited in the EPICA ice core at the MIS 5/4 transition and decrease following the LGM (Fig. 8d), which has been linked to sea ice formation (Wolff et al., 2006; Hansen et al., 2007). Such a change in sea ice formation in the SO would dramatically change the formation of Antarctic Bottom Water (AABW) and thereby dramatically change the deep ocean circulation during the glacial period. This concept bears a close similarity with the conceptual modelling work of Paillard and Parrenin (2004) who developed a simple threshold model to determine the extent of deep water formation in the Southern Ocean during the glacial period. We suggest that such thresholds may in effect drive the bipolar switch.

Alternatively sea ice extent in the high latitude North Atlantic may reduce the formation of North Atlantic Deep Water during the glacial period, reducing the meridional overturning in the Atlantic and the northward heat flux related to it (see for example, Gildor and Tziperman, 2001). Changes to NADW formation may further limit the formation of Antarctic Intermediate Water (AAIW) and promote the formation of AABW during glacial phases. This tallies closely with the results of experiments using the CLIMBER model (Ganopolski and Rahmstorf, 2001) which show that significant changes in the deep circulation of the Atlantic are associated with

the southward migration of deepwater formation zones once the high latitude north Atlantic is insulated from the atmosphere by permanent sea ice. Whether driven from the north Atlantic or SO, thresholds related to sea ice formation seem reasonable candidates to transition the ocean between glacial and modern states and trigger the bipolar switch.

5.3.3. A note on the seasonality hypothesis

A significant alternative explanation to the bipolar switch hypothesis is that the reduced influence of the GL scenario on sea-levels during the glacial period suggested by our model is in fact a result of a seasonal bias in the GL record during the cold periods associated with Heinrich events (Denton et al., 2005). In the case of our model results this implies that the sea-level data require a reduced influence of the NGRIP record because fluctuations in Greenland are actually smaller during the LGM than those suggested by the GL records (which are seasonally biased). However, it is the duration as well as the magnitude of the cold period that drives excessively low sea-levels during MIS 4 in the GL scenario (see Section 4.2.1) because the duration of the cold period dictates the amount of ice sheet growth that can be attained for a given ice sheet response time. This is demonstrated quantitatively in Fig. 5 where the GL scenario features sea-level some tens of meters lower than the AA scenario because of the extended cold period associated with MIS 4 in the GL compared to the AA temperature records. Because the seasonality hypothesis does not have implications for the duration of cold periods but only their magnitude it remains difficult to explain our results using simply the seasonality hypothesis during the glacial period. Instead the bipolar switch must play a role.

Although it is difficult to reconcile our model results with the seasonality hypothesis during MIS 4, this is not the case during T1. During T1 the most important factor influencing the model result is the timing, rather than the magnitude of the warming events associated with the Bolling–Allerød and post Younger Dryas period. This is because sea-level is not at equilibrium during T1 but lags rapid changes in temperature (i.e. the sea-level does not have time to equilibrate with sea-level during T1). The seasonality hypothesis reduces the magnitude of cooling events but does not alter the timing of events and so our model results are consistent with the implications of the seasonality hypothesis during T1.

5.4. Ice sheet contributions

Work is ongoing to identify the ice sheets responsible for sea-level variability during the last glacial cycle. Techniques include sea-level fingerprinting using models of isostatic rebound during the termination (Peltier, 1998; Clark et al., 2002a,b; Bassett et al., 2005). Previous to the termination, attribution techniques include the use of marine oxygen isotope records in the vicinity of the ice sheets as tracers of ice sheet decay (Rohling et al., 2004; Roche et al., 2004) and the direct modelling of ice sheet contributions to sea-level (Marshall and Clarke, 1999; Bintanja et al., 2002, 2005). Although there is consensus on the general proportions of the total ice distribution at the LGM (most of the relative increase in ice volume compared to today was situated over North America and Northern Europe; Peltier, 1998; Bintanja et al., 2002, 2005) the exact contributions are contested and none of the techniques listed here is conclusive. Our modelling results do not attribute changes in sea-level to any particular ice sheet and much further discussion of this issue is beyond the remit of this paper. However the suggestion of Weaver et al. (2003) that the deep ocean circulation was invigorated by a meltwater pulse originating from the Antarctic ice sheet would tally with our results well.

5.5. Limitations of the model – scope for further study

Although our optimal model scenario describes much of the sea-level variability during the LGC, open questions remain. For example, exactly when did the switches occur? The chronology discussed here is based on the events of the termination, rather than their absolute date (i.e. post LGM, MIS 5/4 transition). However, the precise timing and duration of the LGM is only known to within several thousand years, as is the start of the major ice sheet growth during the transition between MIS 4 and 3. Stott et al. (2007) link major warming of the deep Pacific Ocean to warming events in the Southern Ocean which affected deep water formation between ~19 and 17 ka BP. As noted the warming between 20 and 15 ka BP is common to both GL and AA variability (Paillard, 2001; Alley et al., 2002). Although linking the bipolar switch to changes in deep water formation in the Southern Ocean seems reasonable, such a link remains speculative and any timing for the switch taken from such studies relies on the additional assumption of a link between the bipolar switch and deep ocean circulation.

Yokoyama et al. (2000) published evidence for a rapid rise in sea-level of some ten meters or so at 19 ka BP. The simple model presented here captures much of the sea-level variation over the last glacial cycle but is not subtle enough to capture the rapid rise in sea-level at 19 ka BP. This might be because the GL scenario does not include a significant warming at 19 ka BP. The AA scenario based on the EPICA Dome C temperature record does not contain a significant warming at 19 ka BP but Antarctic temperature reconstructions differ on the precise sequence of warming during this period (Brook et al., 2005) and it is possible that our choice of AA record affects our result at 19 ka BP. It is possible that the rapid rise in sea-level at 19 ka BP is a result of the bipolar switch and is missed in our model because the bipolar switch itself is assumed not to affect sea-level at the LGM. We must underline though that the simple model described here does not include the many complexities of ice sheet dynamics (e.g. Marshall and Clarke, 1999; Bintanja et al., 2002; Johnson and Fastook, 2002).

It is possible that the 19 ka event does not relate to temperature reconstructions in a simple way and this is an interesting question to tackle in future studies.

6. Conclusions

We have considered the varying influence of Greenlandic and Antarctic temperature variability during the LGC and TI/H using a minimum-complexity model linking eustatic sea-level to temperature variations. Using ice core temperature data to force the model we are able to represent 95% of the sea-level variability during the LGC and TI/H. This suggests that ice core temperature reconstructions have important implications for broader changes in global climate. That is, our findings support that these two temperature proxies, from Antarctica and Greenland, are representative of changes in regions distant from the poles, in agreement with the findings of Clark et al. (2002a,b, 2007).

We suggest that glacial sea-levels are dominantly controlled by temperature variability characteristic of the AA scenario and sea-levels during interglacial periods/terminations are primarily controlled by temperature variability characteristic of the GL scenario. We call this change in dominance the bipolar switch.

Acknowledgements

Mark Siddall acknowledges support from Lamont Doherty Earth Observatory and the University of Bristol and the PALSEA PAGES/IMAGES working group. Mark Siddall is supported by a Research Council UK fellowship. Helpful suggestions from Thomas Stocker

and John Shepherd have helped to form the ideas in this paper. An insightful and constructive review from Peter Clark was also very useful.

References

- Adkins, J.F., Schrag, D.P., 2003. Reconstructing Last Glacial Maximum bottom water salinities from deep-sea sediment pore fluid profiles. *Earth and Planetary Science Letters* 216, 109–123.
- Adkins, J.F., McIntyre, K., Schrag, D.P., 2002. The salinity, temperature and $\delta^{18}\text{O}$ content of the glacial deep ocean. *Science* 298, 1769–1773.
- Alley, R.B., Brook, E.J., Anandakrishnan, S., 2002. A northern lead in the orbital band: north-south phasing of Ice-Age events. *Quaternary Science Reviews* 21 (1–3), 431–441.
- Alley, R.B., Marotzke, J., Nordhaus, W.D., Overpeck, J.T., Peteet, D.M., Pielke Jr., R.A., Pierrehumbert, R.T., Rhines, P.B., Stocker, T.F., Talley, L.D., Wallace, J.M., 2003. Abrupt climate change. *Science* 299, 2005–2010.
- Andersen, K.K., Svensson, A., Johnsen, S.J., Rasmussen, S.O., Bigler, M., Röhlisberger, R., Ruth, U., Siggaard-Andersen, M.-L., Steffensen, J.-P., Dahl-Jensen, D., Vinther, B.M., Clausen, H.B., 2006. The Greenland Ice Core Chronology 2005, 15–42 ka. Part 1: constructing the time scale. *Quaternary Science Reviews* 25 (23–24), 3246–3257.
- Arz, H.W., Lamy, F., Ganopolski, A., Novaczyk, N., Pätzold, J., 2007. Dominant Northern Hemisphere climate control over millennial-scale sea-level variability. *Quaternary Science Reviews* 26, 312–321.
- Bard, E., Hamelin, B., Arnold, M., Montaggioni, L., Cabioch, G., Faure, G., Rougerie, F., 1996. Sea level record from Tahiti corals and the timing of deglacial meltwater discharge. *Nature* 382, 241–244.
- Barker, S., Knorr, G., 2007. Antarctic climate signature in the Greenland ice core record. *Proceedings of the National Academy of Science USA* 104, 17278–17282.
- Basile, I., Grousset, F.E., Revel, M., Petit, J.R., Biscaye, P.E., Barkov, N.I., 1997. Patagonian origin of glacial dust deposited in East Antarctica (Vostok and Dome C) during glacial stages 2, 4, and 6. *Earth and Planetary Science Letters* 146, 573–589.
- Bassett, S.E., Milne, G.A., Mitrovica, J.X., Clark, P.U., 2005. Ice sheet and solid earth influences on far-field sea-level histories. *Science* 309, 925–928.
- Bintanja, R., van de Wal, R.S.W., 2008. A three million-year history of Northern Hemisphere glaciation. *Nature* 454, 869–872. doi:10.1038/nature0715.
- Bintanja, R., van de Wal, R.S.W., Oerlemans, J., 2002. Global ice volume variations through the last glacial cycle simulated by a 3-D ice-dynamical model. *Quaternary International* 95–96, 11–23.
- Bintanja, R., van de Wal, R.S.W., Oerlemans, J., 2005. Modelled atmospheric temperatures and global sea levels over the past million years. *Nature* 437, 125–128.
- Blunier, T., Brook, E., 2001. Timing of millennial-scale climate change in Antarctica and Greenland during the last glacial period. *Science* 291, 109–112.
- Blunier, T., Chappellaz, J., Schwander, J., Dällenbach, A., Stauffer, B., Stocker, T.F., Raynaud, D., Jouzel, J., Clausen, H.B., Hammer, C.U., Johnsen, S.J., 1998. Asynchrony of Antarctica and Greenland climate during the last glacial. *Nature* 394, 739–743.
- Brook, E., White, J.W.C., Schilla, A., Bender, M., Barnett, B.A., Severinghaus, J., Taylor, K.C., Alley, R.B., Steig, E.J., 2005. Timing of millennial-scale climate change at Siple Dome, West Antarctica, during the last glacial period. *Quaternary Science Reviews* 24, 1333–1343.
- Budd, W.F., Smith, I.N., 1979. The growth and retreat of ice sheets in response to orbital radiation changes. *International Association of Hydrological Sciences. Publication no. 131*, 369–409.
- Chappell, J., 2002. Sea level changes forced ice breakouts in the Last Glacial Cycle: new results from coral terraces. *Quaternary Science Reviews* 21 (10), 1229–1240.
- Chappell, J., Shackleton, N.J., 1986. Oxygen isotopes and sea-level. *Nature* 324 (6093), 137–140.
- Clark, P.U., 2002a. Early deglaciation in the tropical Andes. *Science*, v.298.
- Clark, P.U., Mitrovica, J.X., Milne, G.A., Tamisiea, M., 2002b. Sea-level fingerprinting as a direct test for the source of global meltwater pulse 1A. *Science* 295, 2438–2441.
- Clark, P.U., Pisias, N.G., Stocker, T.F., Weaver, A.J., 2002c. The role of the thermohaline circulation in abrupt climate change. *Nature* 415, 863–869.
- Clark, P.U., 2002. Early deglaciation in the tropical Andes. *Science*, 298.
- Clark, P.U., Hostetler, S.W., Pisias, N.G., Schmittner, A., Meissner, K.J., 2007. Mechanisms for a ~7-kyr climate and sea-level oscillation during Marine Isotope Stage 3. In: *Ocean Circulation: Mechanisms and Impacts*, Geophys. Monograph Ser. 173. American Geophysical Union 249–246.
- Curry, W.B., Oppo, D.W., 2005. Glacial water mass geometry and the distribution of $\delta^{13}\text{C}$ of SeCO_2 in the Western Atlantic Ocean. *Paleoceanography*. doi:10.1029/2004PA001021.
- Cutler, K.B., Edwards, R.L., Taylor, F.W., Cheng, H., Adkins, J., Gallup, C.D., Cutler, P.M., Burr, G.S., Bloom, A.L., 2003. Rapid sea-level fall and deep-temperature change since the last interglacial period. *Earth and Planetary Science Letters* 206 (3–4), 253–271.
- Dansgaard, W., Johnsen, S.J., Clausen, H.B., Dahl-Jensen, D., Gundestrup, N., Hammer, C.U., Oeschger, H., 1984. North Atlantic climatic oscillations revealed by deep Greenland ice cores. In: Hansen, J.E., Takahashi, T. (Eds.), *Climate Processes and Climate Sensitivity*, Geophys. Monogr. Ser., 29. AGU, Washington, D.C., pp. 288–298.

- Dansgaard, W., Johnsen, S.J., Clausen, H.B., Dahl-Jensen, D., Gundestup, N.S., Hammer, C.U., Hvidberg, C.S., Steffensen, J.P., Sveinbjornsdottir, A.E., Jouzel, J., Bond, G., 1993. Evidence for general instability of past climate from a 250-ka ice-core record. *Nature* 364, 218–220.
- Denton, G.H., 2000. Does an asymmetric thermohaline-ice-sheet oscillator drive 100 000-yr glacial cycles? *Journal of Quaternary Science* 15 (4), 301–318.
- Denton, G.H., Lowell, T.V., Heusser, C.J., Moreno, P.I., Andersen, B.G., Heusser, L.E., Schlüchter, C., Marchant, D.R., 1999. Interhemispheric linkage of paleoclimate during the last glaciation. *Geografiska Annaler* 81, 107–153.
- Denton, G.H., Alley, R.B., Comer, G.C., Broecker, W.S., 2005. The role of seasonality in abrupt climate change. *Quaternary Science Reviews* 24 (10–11), 1159–1182.
- Dyke, A.S., Andrews, J.T., Clark, P.U., England, J.H., Miller, G.H., Shaw, J., Veillette, J.J., 2002. The Laurentide and Innuitian ice sheets during the Last Glacial Maximum. *Quaternary Science Reviews* 21 (1–3), 9–31.
- EPICA Members, 2004. Eight glacial cycles from an Antarctic ice core. *Nature* 429, 623–628.
- EPICA Members, 2006. One-to-one coupling of glacial climate variability in Greenland and Antarctica. *Nature* 444, 195–198.
- Fairbanks, R.G., 1989. A 17,000 year glacio-eustatic sea level record: influence of glacial melting rates on the Younger Dryas event and deep ocean circulation. *Nature* 342, 637–642.
- Fleming, K., Johnston, P., Zwart, D., Yokoyama, Y., Lambeck, K., Chappell, J., 1998. Refining the eustatic sea-level curve since the Last Glacial Maximum using far-and intermediate-field sites. *Earth and Planetary Science Letters* 163 (1–4), 327–342. doi:10.1016/S0012-821X(98)00198-8.
- Ganopolski, A., Rahmstorf, S., 2001. Simulation of rapid glacial climate changes in a coupled climate model. *Nature* 409, 153–158.
- Gildor, H., Tziperman, E., 2001. A sea-ice climate-switch mechanism for the 100 kyr glacial cycles. *Journal of Geophysical Research-Oceans* 106 (C5), 9117–9133.
- Hanebuth, T., Statteger, K., Grootes, P.M., 2000. Rapid flooding of the Sunda Shelf: a late-glacial sea-level record. *Science* 288 (5468), 1033–1035. doi:10.1126/science.288.5468.1033.
- Hansen, J., Sato, M., Karecha, P., Russel, G., Lea, D.W., Siddall, M., 2007. Climate change and trace gases. *Philosophical Transactions of the Royal Society A* 365, 1925–1954.
- Hemming, S.R., 2004. Heinrich events: massive late Pleistocene detritus layers of the North Atlantic and their global imprint. *Reviews of Geophysics* 42, RG1005. doi:10.1029/2003RG000128.
- Imbrie, J., Hays, J.D., Martinson, D.G., McIntyre, A., Mix, A.C., Morley, J.J., Pisias, N.G., Prell, W.L., Shackleton, N.J., 1984. The orbital theory of Pleistocene climate: support from a revised chronology of the marine $\delta^{18}\text{O}$ record. In: Berger, A.L., Imbrie, J., Hays, J., Kukla, G., Saltzman, B. (Eds.), *Milankovitch and Climate*, Part 1. D. Reidel, Reidel, pp. 269–305.
- IPCC, 2007. Summary for policymakers. In: Solomon, S., Qin, D., Manning, M., Chen, Z., Marquis, M., Averyt, K.B., Tignor, M., Miller, H.L. (Eds.), *Climate Change 2007: The Physical Science Basis*. Contribution of Working Group I to the Fourth Assessment Report of the Intergovernmental Panel on Climate Change. Cambridge University Press, Cambridge, United Kingdom and New York, NY, USA.
- Johnson, J., Fastook, J.L., 2002. Northern Hemisphere glaciation and its sensitivity to basal melt water. *Quaternary International* 95 (6), 65–74. PII S1040-6182(02)00028-9.
- Jouzel, J., et al., 2007. Orbital and millennial Antarctic climate variability over the past 800,000 years. *Science* 317 (5839), 793–797. doi:10.1126/science.1141038.
- Kawamura, K., et al., 2007. Northern Hemisphere forcing of climatic cycles in Antarctica over the past 360,000 years. *Nature* 448, 912–916.
- Knutti, R., Flückiger, J., Stocker, T.F., Timmermann, A., 2004. Strong hemispheric coupling of glacial climate through freshwater discharge and ocean circulation. *Nature* 430, 851–856. doi:10.1038/nature02786.
- Lambeck, K., Yokoyama, Y., Purcell, A., 2002. Into and out of Last Glacial Maximum: sea-level change during the Oxygen Isotope Stage 3 and 2. *Quaternary Science Reviews* 21, 343–360.
- Lea, D.W., Martin, P.A., Pak, D.K., Spero, H.J., 2002. Reconstructing a 350 ky history of sea level using planktonic Mg/Ca and oxygen isotope records from a Cocos Ridge core. *Quaternary Science Reviews* 21, 283–293.
- Lear, C.H., Elderfield, H., Wilson, P.A., 2000. Cenozoic deep-sea temperatures and global ice volumes from Mg/Ca in benthic foraminiferal calcite. *Science* 287, 269–272.
- Lowell, T.V., 1995. The application of radiocarbon age estimates to the dating of glacial sequences: an example from the Miami sublobe, Ohio. *Quaternary Science Reviews* 14, 85–94.
- Lowell, T.V., Heusser, C.J., Anderson, B.G., Moreno, P.I., Hauser, A., Huessler, L.E., Schlüchter, C., Marchant, D.R., Denton, G.H., 1995. Interhemispheric correlation of late Pleistocene glacial events. *Science* 269, 1541–1549.
- Marshall, S.J., Clarke, G.K.C., 1999. Modeling North American freshwater runoff through the last glacial cycle. *Quaternary Research* 52 (3), 300–315.
- Martinson, D.G., Pisias, N.G., Hays, J.D., Imbrie, J., Moore Jr., T.C., Shackleton, N.J., 1987. Age dating and the orbital theory of the ice ages development of a high-resolution 0 to 300 000-year chronostratigraphy. *Quaternary Research* 27, 1–29.
- Masson-Delmotte, V., et al., 2006. Past and future polar amplification of climate change: climate model intercomparisons and ice-core constraints. *Climate Dynamics* 26 (5), 513–529.
- McManus, J.F., Oppo, D.W., Cullen, J.L., 1999. A 0.5-million-year record of millennial-scale climate variability in the North Atlantic. *Science* 283 (5404), 971–975.
- Milne, G.A., Mitrovica, J.X., Schrag, D.P., 2002. Estimating past continental ice volume from sea-level data. *Quaternary Science Reviews* 21 (1–3), 361–376.
- MIS 8 millennial variability stratigraphically identical to MIS 3, *Paleoceanography*, 22, No. 1, PA120810.1029/2006PA00134.
- Mix, A.C., Ruddiman, W.F., 1984. Oxygen-isotope analyses and Pleistocene ice volumes. *Quaternary Research* 21, 1–20.
- Muhs, D.R., 2002. Evidence for the timing and duration of the last interglacial period from high-precision uranium-series ages of corals on tectonically stable coastlines. *Quaternary Research* 58 (1), 36–40.
- Murray-Wallace, C.V., 2002. Pleistocene coastal stratigraphy, sealevel highstands and neotectonism of the southern Australian passive continental margin – a review. *Journal of Quaternary Science* 17 (5–6), 469–489.
- NGRIP members, 2004. High-resolution record of Northern Hemisphere climate extending into the last interglacial period. *Nature* 431, 147–151.
- Oerlemans, J., 1991. The role of ice sheets in the Pleistocene climate. *Norsk Geologisk Tidsskrift* 71, 155–161.
- Oeschger, H., Beer, J., Siegenthaler, U., Stauffer, B., Dansgaard, W., Langway, C.C., 1984. Late glacial climate history from ice cores. In: Hansen, J.E., Takahashi, T. (Eds.), *Climate Processes and Climate Sensitivity*, Geophysical Monograph Series, vol. 29. AGU, Washington, DC, pp. 299–306.
- Oppo, D.W., McManus, J.F., Cullen, J.L., 1998. Abrupt climate events 500,000 to 340,000 years ago: evidence from subpolar north Atlantic sediments. *Science* 279 (5355), 1335–1338.
- Paillard, D., 2001. Glacial cycles: towards a new paradigm. *Reviews of Geophysics* 39 (3), 325–346.
- Paillard, D., Parrenin, F., 2004. The Antarctic ice sheet and the triggering of deglaciations. *Earth and Planetary Science Letters* 227 (3–4), 263–271.
- Pailler, M., Bard, E., 2002. High-frequency paleoceanographic changes during the past 140,000 years recorded by the organic matter in sediments off the Iberian Margin. *Paleogeography, Paleoclimatology, Paleoecology* 181, 431–452.
- Peltier, W., 1998. Postglacial variations in the level of the sea: implications for climate dynamics and solid-earth geophysics. *Reviews of Geophysics* 36 (4), 603–689.
- Peltier, W.R., Fairbanks, R.G., 2006. Global glacial ice volume and Last Glacial Maximum duration from an extended Barbados sea level record. *Quaternary Science Reviews* 25, 3322–3337.
- Petit, J.R., et al., 1999. Climate and atmospheric history of the past 420,000 years from the Vostok Ice Core, Antarctica. *Nature* 399, 429–436.
- Pirazzoli, P.A., Raddtke, U., Hantoro, W.S., Jouannic, C., Hoang, C.T., Causse, C., Borel Best, M., 1991. Quaternary raised coral-reef terraces on Sumba Island, Indonesia. *Science* 252, 1834–1836.
- Rahmstorf, S., 2007. A semi-empirical approach to projecting future sea-level rise. *Science* 315, 368–370.
- Roche, D., Paillard, C., Cortijo, E., 2004. Constraints on the duration and freshwater release of Heinrich event 4 through isotope modelling. *Nature* 432 (7015), 379–382. doi:10.1038/nature03059.
- Rohling, E.J., Fenton, M., Jorissen, F.J., Bertrand, P., Ganssen, G., Caulet, J.P., 1998. Magnitudes of sea-level lowstands of the past 500,000 years. *Nature* 394, 162–165.
- Rohling, E.J., Marsh, R., Wells, N.C., Siddall, M., Edwards, N.R., 2004. Similar meltwater contributions to glacial sea level changes from Antarctic and northern ice sheets. *Nature* 430, 1016–1102.
- Rohling, E.J., Grant, K., Hemleben, Ch., Kucera, M., Roberts, A.P., Schmeltzer, I., Schulz, H., Siccha, M., Siddall, M., Trommer, G., 2008. New constraints on the timing and amplitude of sea level fluctuations during Marine Isotope Stage 3. *Paleoceanography* 23, PA3219. doi:10.1029/2008PA001617.
- Rohling, E.J., Grant, K., Bolshaw, M., Roberts, A.P., Siddall, M., Hemleben, Ch., Kucera, M., 2009. Antarctic temperature and global sea level closely coupled over the past five glacial cycles. *Nature Geoscience* 2, 500–504.
- Schellmann, G., Raddtke, U., 2004. A revised morphoand chronostratigraphy of the late and middle Pleistocene coral reef terraces on Southern Barbados (West Indies). *Earth-Science Reviews* 64, 157–187.
- Schmittner, A., Saenko, O.A., Weaver, A.J., 2003. Coupling of the hemispheres in observations and simulations of glacial climate change. *Quaternary Science Reviews* 22 (5–7), 659–671.
- Shackleton, N.J., 1974. Attainment of isotopic equilibrium between ocean water and benthic foraminifera genus *Uvigerina*: isotopic changes in the ocean during the last glacial. *Les méthodes quantitatives d'étude des variations du climat au cours du Pleistocène*, Gif-sur-Yvette. Colloque international du CNRS 219, 203–210.
- Shackleton, N.J., Berger, A., Peltier, W.R., 1990. An alternative astronomical calibration on the lower Pleistocene time scale based on ODP site 677. *Transactions of the Royal Society of Edinburgh. Earth Science* 81, 2511–261.
- Shackleton, N.J., Hall, M.A., Vincent, E., 2000. Phase relationships between millennial-scale events 64,000–24,000 years ago. *Paleoceanography* 15, 565–569.
- Siddall, M., Rohling, E.J., Almogi-Labin, A., Hemleben, Ch., Meischner, D., Schmelzer, I., Smeed, D.A., 2003. Sea-level fluctuations during the last glacial cycle. *Nature* 423, 853–858.
- Siddall, M., Rohling, E.J., Smeed, D.A., Hemleben, Ch., Meischner, D., 2004. Understanding the Red Sea response to sea level. *Earth and Planetary Science Letters* 225, 421–434.
- Siddall, M., Stocker T.F., Blunier T., Spahni R., Schwander J., Barnola J.-M., Chappellaz, J., 2007. MIS 8 millennial variability stratigraphically identical to MIS 3. *Paleoceanography*, 22, PA1208. doi:10.1029/2006PA001345.
- Siddall, M., Rohling, E.J., Arz, H.W., 2008a. Convincing evidence for rapid ice sheet growth during the last glacial period. *PAGES newsletter* 16 (1), 15–16.

- Siddall, M., Rohling, E.J., Thompson, W.G., Waelbroeck, C., 2008b. MIS 3 sea-level fluctuations: data synthesis and new outlook. *Reviews of Geophysics*, in press.
- Siddall, M., Stocker, T.F., Clark, P.U., 2009d. Constraints on future sea level rise from paleo reconstructions. *Nature Geoscience* 2, 571–575.
- Siddall, M., Hönisch, B., Waelbroeck, C., Huybers, P., 2009a. Changes in deep Pacific temperature during the mid-Pleistocene transition and Quaternary. *Quaternary Science Reviews* 29 (1–2), 170–181.
- Siddall, M., Stocker, T.F., Clark, P.U., 2009b. Paleo-constraints on future sea-level rise. *Nature Geoscience* 2, 571–575.
- Stirling, C.H., Esat, T.M., Lambeck, K., McCulloch, M.T., 1998. Timing and duration of the last interglacial: evidence for a restricted interval of widespread coral reef growth. *Earth and Planetary Science Letters* 160, 745–762.
- Stocker, T.F., Johnsen, S.J., 2003. A minimum model for the bipolar seesaw. *Paleoceanography* 18 (1087). doi:10.1029/2003PA000920.
- Stott, L.D., Timmermann, A., Thunell, R., 2007. Deep sea temperatures warmed before atmospheric CO₂ and tropical temperatures began to rise at the last glacial termination. *Science* 318 (435).
- Svensson, A., Andersen, K.K., Bigler, M., Clausen, H.B., Dahl-Jensen, D., Davies, S.M., Johnsen, S.J., Muscheler, R., Rasmussen, S.O., Röthlisberger, R., Steffensen, J.-P., Vinther, B.M., 2006. The Greenland Ice Core Chronology 2005, 15–42 ka. Part 2: comparison to other records. *Quaternary Science Reviews* 25 (23–24), 3258–3267.
- Thompson, W.G., Goldstein, S.L., 2005. Open-system coral ages reveal persistent suborbital sea-level cycles. *Science* 308 (5720), 401–404.
- Thompson, W.G., Goldstein, S.L., 2006. A radiometric calibration of the SPECMAP timescale. *Quaternary Science Reviews* 25 (23–24), 3207–3215.
- Vimeux, F., Masson, V., Delaygue, G., Jouzel, J., Petit, J.R., Stievenard, M., 2001. A 420,000 year deuterium excess record from East Antarctica: information on past changes in the origin of precipitation at Vostok. *Journal of Geophysical Research-Atmospheres* 106 (D23), 31863–31873.
- Waelbroeck, C., Labeyrie, L., Michel, E., Duplessy, J.C., McManus, J.F., Lambeck, K., Balbon, E., Labracherie, M., 2002. Sea-level and deep water temperature changes derived from benthonic foraminifera isotopic records. *Quaternary Science Reviews* 21, 295–305.
- Wang, Y.J., Cheng, H., Edwards, R.L., An, Z.S., Wu, J.Y., Shen, C.C., Dorale, J.A., 2001. A high-resolution absolute-dated Late Pleistocene monsoon record from Hulu Cave, China. *Science* 294 (5550), 2345–2348.
- Weaver, A.J., Saenko, O.A., Clark, P.U., Mitrovica, J.X., 2003. Meltwater pulse 1A from Antarctica as a trigger of the Bolling–Allerod warm period. *Science* 299, 1709–1713.
- Weertman, J., 1964. The theory of glacier sliding. *Journal of Glaciology* 5 (39), 287–303.
- Wolff, E.W., et al., 2006. Southern Ocean sea-ice extent, productivity and iron flux over the past eight glacial cycles. *Nature* 440, 491–496.
- Yokoyama, Y., Lambeck, K., De Deckker, P., Johnston, P., Fifield, L.K., 2000. Timing of the Last Glacial Maximum from observed sea-level minima. *Nature* 406 (6797), 713–716.